

INTERNATIONAL CLIMATE INITIATIVE

Regional project

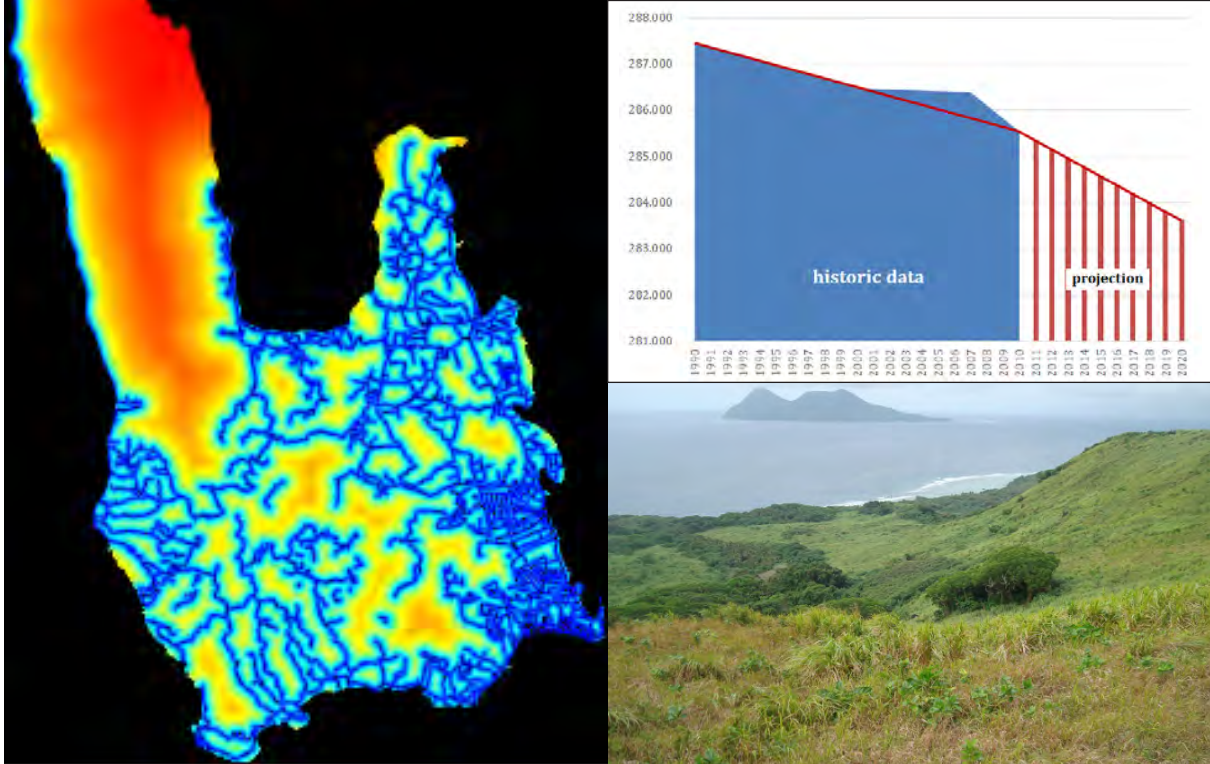
Climate Protection through Forest Conservation in Pacific Island Countries

On behalf of:



Federal Ministry
for the Environment, Nature Conservation,
Building and Nuclear Safety

of the Federal Republic of Germany



Historical and projected deforestation rates 1990 -2020 for Santo Island / Vanuatu

Processing description and results



SPC
Secretariat
of the Pacific
Community

giz Deutsche Gesellschaft
für Internationale
Zusammenarbeit (GIZ) GmbH

Historical and projected deforestation rates 1990 -2020 for Santo Island / Vanuatu

Processing description and results

April, 15 2014



On behalf of:



of the Federal Republic of Germany

Prepared by:

Jörg Seifert-Granzin
Dorys Mendez Zeballos
Email: jseifert@mesa-consult.com



On behalf of:

SPC/GIZ Regional Project
'Climate Protection through Forest Conservation in Pacific Island Countries'
P.O. Box 14041, SUVA, Fiji
Email: karl-peter.kirsch-jung@giz.de

Executive summary

The island of Santo in the Republic of Vanuatu has a forest cover of 285,530 ha (2010). In a pilot modelling approach, a forest cover change projection for the years of 2010 - 2020 has been developed. This will inform the process of developing a reference emission level (REL) for the forest sector in Vanuatu.

The model predicts a total deforestation of 1,898.8 ha or 0.67% for the period 2011-2020, as shown on the map on page 26. The average annual deforestation rate therefore remains low at 0.067%, or ca. 190 ha per year. Most of the deforestation will occur in the surroundings of the provincial capital Luganville and, to a lesser extent, along Santo's west coast. The highest impact on forest carbon is assumed to come from forest degradation, which could not be included in this analysis due to lack of data.

While the projected rate is twice as high as the historically measured deforestation between 1990 and 2010 (0.33 % - 1,907.1 ha), it remains significantly below the observed 2007 – 2010 deforestation (0.1% - 854.7 ha). The approach, as described in chapter 1, combines three types of data sets:

1. Remote sensing data and results covering different periods have been used to reconstruct the deforestation trajectory for the periods 1990-2000, 2000-2007, and 2007-2010;
2. The National Census of Population and Housing data and the Agricultural Census data published by Vanuatu's National Statistics Office served as a basis to conclude which drivers and underlying causes have to be considered in projecting the future deforestation trajectory;
3. Data to model settlement patterns, road networks, and landscape features was used to develop the driver proxies.

In future work steps, the quality of the inputs has to be improved in order increase the accuracy and acceptance of this conservatively developed deforestation baseline. However, this information will provide the government of Vanuatu with a basic understanding of the pattern of deforestation dynamics in Santo: the island can be divided into two sub-regions. While deforestation on Santo's west coast is driven by small scale agriculture and small-scale agricultural trade relying on shipping, land-use change in Santo's eastern part is driven by cattle ranching, medium scale agriculture, urbanization, and tourism development. This has to be considered when developing concrete incentives to stop deforestation.

Apart from the process of developing a reference level for future greenhouse gas emissions from the forest sector in a province of Vanuatu, the report points to an issue which has to be considered by all Pacific Island Countries: While continental areas are usually covered by the LandsAT 8 satellite at around two scenes per month during the last 11 months, Vanuatu to date has been covered by 7 scenes only. A similar rate can be assumed for most countries in the region. It is of utmost importance for the sustainability of the National Forest Monitoring Systems, that the Governments of the Region request USGS to cover the small island states in the same way as the continental areas.

Contents

Executive summary	3
Introduction	6
1 Conceptual approach, methods, and data to model land cover and land-use change.....	7
1.1 The foundations of land use and land cover change modeling.....	7
1.2 The spatial modeling approach.....	8
1.3 Available data sets	9
2 Projecting future deforestation using Dinamica EGO	11
2.1 Overview on the processing chain	11
2.2 Processing steps	12
3 Discussion of results	23
4 Recommendations.....	26
4.1 Improvements of the change detection processing chains.....	26
4.2 Improvements of the modeling approach	27
4.3 Priorities for REL development.....	27
References.....	28
Annex 1: Transition matrices for different deforestation periods	31
Annex 2: Correlation of driver proxies.....	32

List of tables

Table 1: Proxies and related drivers/causes.....	14
Table 2: Deforestation rates and demographic growth 1990 – 2010.....	23
Table 3: Comparison of total and annual area; total and annual rate of deforestation in Santo Island for the observed and projected periods.....	25

List of figures

Figure 1: Drivers and underlying causes of deforestation.....	8
Figure 2: Model and results of the transition matrix for the period 1990-2010.....	12
Figure 3: Distance map processing applied to the provincial capital	13
Figure 4: Configuration of the Determine the Weights of Evidence Ranges Functor	18
Figure 5: Visual interpretation of the significance of WoE coefficients	19
Figure 6: Configuration of the correlation assessment model.....	20
Figure 7: LULCC simulation model for the period 1990 - 2000.....	20
Figure 8: Deforestation probability map for year 2010.....	21
Figure 9: Similarity assessment for period 1990 - 2000	21
Figure 10: Similarity between simulated and observed deforestation for the period 1990 - 2000.....	22
Figure 11: Deforestation projection model 1990 - 2020	23
Figure 12: Projected 2020 forest cover and 2011 – 2020 deforestation.....	24
Figure 13: Historic and projected forest cover change on Espiritu Santo Island, 1990 – 2020.....	25

Acronyms

DoF	Vanuatu Department of Forestry
DSM	Digital Surface Model
FBD	Fine resolution model dual polarization
FNF	Forest/non-forest
GOFC-GOLD	Global Observation of Forest and Land Cover Dynamics
IPCC	Intergovernmental Panel on Climate Change
JAXA	Japan Aerospace Exploration Agency
K&C3	3rd Kyoto and Carbon Science Program
LCC	Land cover change
LULCC	Land-use / land-cover change
LULUCF	Land Use, Land-Use Change, and Forestry
MMU	Minimum mapping unit
MRV	Measurement, reporting, and verification
REDD+	Reducing emissions from deforestation, forest degradation, conservation, sustainable management of forests and enhancement of carbon stocks
RS	Remote sensing
SAR	Synthetic Aperture Radar (SAR)
SBSTA	Subsidiary Body on Scientific and Technological Advice
SRTM	Shuttle Radar Topography Mission
UNFCCC	United Nations Framework Convention on Climate Change
VHR	Very-high resolution (VHR) optical data
WGS	World Geodetic System

Introduction

Reducing emissions from deforestation, forest degradation, sustainable management of forests, enhancement and conservation of forest carbon stocks (REDD+) is considered one of the most cost-effective options to mitigate climate change. The Conference of the Parties (COP) to the United Nations Framework Convention on Climate Change (UNFCCC) frames REDD+ as one of the building blocks of the post-Kyoto mitigation architecture negotiated in the Ad-hoc Working Group on Long-term Cooperative Action (AWG-LCA) and The Subsidiary Body on Scientific and Technological Advice (SBSTA). While negotiations on measurement, reporting and verification (MRV) of greenhouse gas emission reductions and Removals (ERR) haven't been concluded, the modalities for establishing reference (emission) levels and for informing on safeguards compliance have been agreed. The Cancún-Agreements frame REDD+ implementation as a phased approach: Countries are requested to develop their REDD+ strategies or action plans to defined policies to be implemented in the second phase involving capacity building, technology development and results-based demonstration activities, evolving into results-based actions that should be fully measured, reported and verified during the third phase (1/CP.16 par. 73 in FCCC/CP/2010/7/Add.1). Convened in November 2013 in Warsaw, COP 19 consolidated the modalities for developing National Forest Monitoring Systems (NFMS), for MRV, and for the technical assessment of Forest Reference Emission Levels and Forest Reference Levels (FREL/FRL), which together with other decisions form the so-called *Warsaw Framework for REDD-plus* (FCCC/CP/2013/10, par. 44).

The term “reference level” refers to a scenario providing emission levels over an agreed period of time to be used as benchmark to measure performance of forest and land-use policy adjustments (Brown et al. 2006). Such benchmarks are constructed combining information (so-called “activity data”) on the magnitude of anthropogenic interventions causing greenhouse gas (GHG) emissions (e.g. deforestation patterns of a predefined period in the past) with information (so-called “emission factors”) representing different forest carbon pools (Meridian Institute 2011b). In case of forests, these pools include above-ground and below-ground biomass, litter, soil carbon, dead wood, and harvested wood products (Eggleston et al. 2006). Then, historic activity data is extrapolated into the future to develop a business-as-usual (BAU) scenario to be used as a benchmark. It is common practice to use spatial modeling to locate areas under risk to be deforested in the future (VCS 2013).

As of now, only a few countries have presented a reference emission level for REDD+¹. While several methodologies have been developed and successfully tested in project-based approaches focusing on voluntary markets², subnational and national implementation of REDD+ faces particular challenges related to scale, policies and complexity (Meridian Institute 2011b; Meridian Institute 2011a). Land-use change detection covering a national territory in a wall-to-wall mode across several periods has to deal with data gaps due to clouds, or missing sensor coverage or ground truth data (GOF-C-GOLD 2013). Heterogeneous sensor products have to be processed and integrated and the capabilities of new sensor systems (e.g. Landsat 8, Sentinel-1/2, ALOS Palsar 2, CBERS 4) have to be anticipated in setting up national forest monitoring systems.

The impacts of policies on the dynamics of land-use change are difficult to assess. Bridging the gap between observed deforestation patterns and fragmented socio-economic data applying conceptual models of drivers, underlying causes and agents of deforestation (Geist and Lambin 2001; Geist and Lambin 2002) at the national level remains a challenge. Consequently, land-use change models providing a business-as-usual scenario for the near future, which is supposed to be counterfactual, rely to a certain extent on expert judgment. Expert judgment needs to be flagged following agreed standards established by the IPCC (Penman et al. 2003). Complementarily, the validation of reference emission levels and its input data requires agreed

¹ The Forest Carbon Partnership Facility (FCPF) of the World Bank (<http://www.forestcarbonpartnership.org/fcp/>) and the UN-REDD, REDD Program of the United Nations (<http://www.un-redd.org/>) maintain databases documenting countries' achievements in implementing REDD+.

² The REDD+ methodologies certified under the Verified Carbon Standard are available at www.v-c-s.org.

methods, too. The UNFCCC parties have addressed these issues in several workshops (FCCC/SBSTA/2006/10; FCCC/SBSTA/2009/2³) and concluded on guidelines and procedures for the technical assessment of FREL/FRLs (Decision 13/CP.19 in FCCC/CP/2013/10/Add.1).

Small-island states face particular challenges in establishing their reference level. Their national territory is discontinuous, composed of islands differing in size, vegetation, socio-economic development, and topography. Poor satellite coverage, cloud cover, and rough topography hampered land-use change monitoring in the past. In its REDD+ Strategy, Vanuatu, a Pacific island country, commits to a subnational REDD+ implementation mode. The German Environment Ministry, facilitated by the Gesellschaft für Internationale Zusammenarbeit (GIZ), is supporting Vanuatu's REDD+ process with its regional Project "*Climate Protection through Forest Conservation in the Pacific Island Countries*". As Vanuatu's provincial boundaries encompass several islands differing in size, and the dynamics of drivers of deforestation and forest degradation, a subnational REL design based on island topography is currently being considered to be piloted on Santo Island. A REL is based on historic deforestation patterns and rates across several periods (e.g. 1990-2000-2007-2010). As Vanuatu has been poorly covered by medium resolution multispectral optical sensors in the past, optical processing has to be combined with Synthetic Aperture Radar (SAR) data processing to derive cloud-free forest masks (Herold et al. 2007). While multi-sensor approaches have been successfully tested in large scale forest cover classification and mapping (Walker et al. 2010), methodological guidance on multi-temporal multi-sensor integration in small to medium scale forest-cover mapping is scarce.

Within this context, this processing note describes how to develop a subnational forest reference emission level for Espiritu Santo Island, Vanuatu, using a spatial modeling approach. Section 1 describes its conceptual framework, methods, and data used in this analysis. Section 2 describes the processing steps applied in the spatial projection of the future deforestation pattern. Section 3 discusses the preliminary results. The technical note concludes with recommendations how to proceed in closing data gaps and how to develop the model further.

1 Conceptual approach, methods, and data to model land cover and land-use change

1.1 The foundations of land use and land cover change modeling

Land use / land cover (LULC) change refers to "(quantitative) changes in the areal extent (increases or decreases) of a given type of land use or land cover" (Briassoulis 2001). The system of the IPCC is particularly useful in this context as it covers all potential transitions between different LULC categories within a generic approach (Eggleston et al. 2006). However, within its reporting perspective IPCC focusses on anthropogenic change, while LULC might be caused by natural events (extreme weather events, geo-hazards) as well.

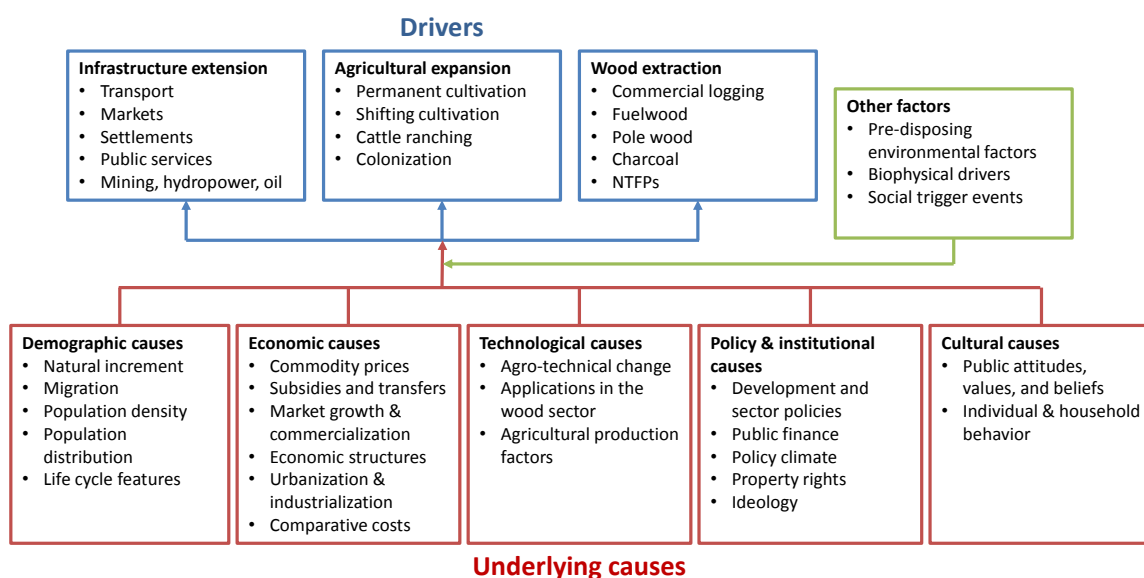
Early research in computational modelling of tropical land use change already referred to underlying driving forces (Turner II, Skole, and Meyer 1994) or pattern drivers (Hall et al. 1995), but did not embed their analysis in an explicit conceptual framework or unifying theory of land use change. The work of Geist and Lambin on proximate and underlying causes of deforestation (Geist and Lambin 2001; Geist and Lambin 2002) can be considered the starting point of a systematic conceptual approach towards building a unifying theory of land use change. The authors base their conceptual framework on the distinction of proximate causes and underlying driving forces (Geist and Lambin 2002). Proximate causes are introduced as "human activities or immediate actions at the local level [...] that originate from intended land use and directly impact forest cover", while underlying driving forces are framed as "fundamental social processes [...] that underpin the proximate causes and either operate at the local level or have indirect impact from the national or global level" (ibid). Geist and Lambin developed a comprehensive view clustering potential proximate causes and

3 Official UN documents and decisions are referenced by their official symbol. The UNFCCC documents are available at: <http://unfccc.int/documentation/documents/items/3595.php>.

underlying driving forces (cf. figure 1). The idea of underlying forces (or “causes”) driving proximate causes (“drivers”) has been widely anticipated in REDD+ research and, to a lesser extent, in REDD+ negotiations⁴.

LULCC models capture the interaction between anthropogenic driver, causes, agents and natural systems in space and time. During the last decade, several LULCC modeling techniques have emerged and were reviewed by the LULCC science and user community (Briassoulis 2001; Agarwal et al. 2002; Verburg et al. 2004; Schaldach and Priess 2008; Committee on Needs and Research Requirements for Land Change Modeling et al. 2013). Within the REDD+ developer and user community, cellular automaton based approaches⁵ are widely used to establish forest reference emission levels for reducing deforestation (Brown et al. 2006; Leite et al. 2012).

Figure 1: Drivers and underlying causes of deforestation



Source: Geist and Lambin 2002 (adapted)

1.2 The spatial modeling approach

Amongst the LULCC modeling approaches used in the REDD+ community, Dinamica Environment for Geoprocessing Objects (EGO) has an outstanding trajectory. Dinamica EGO is an environmental modeling framework developed by the Remote Sensing lab of the Universidade Federal de Minas Gerais, Brazil⁶. It is being used all over the world to assess landscape and LULCC dynamics (Britaldo Silveira Soares-Filho et al. 2006; Maeda et al. 2010; Thapa and Murayama 2011; Yi et al. 2012; Carlson et al. 2012). The modeling suite has proven to be more open, faster, and more flexible than similar modeling environments (Mas et al. 2014).

Dinamica EGO applies a Bayesian Statistics approach implemented by the so-called Weights of Evidence (WoE) method (B. S. Soares-Filho, Rodrigues, and Costa 2013). The approach requires a transition matrix

⁴ The Warsaw Framework for REDD-plus only recognizes “that drivers of deforestation and forest degradation have many causes” (Decision 15/CP.19 in FCCC/CP/2013/10/Add.1, par. 2), but doesn’t elaborate further on how to address them.

⁵ Cellular automata refer to a broad class of modeling techniques in which space is represented as a regular grid of homogenous cells which can assume certain predefined states determined by a set of rules at any time step anticipating the state of neighboring cells. This technique can be considered the workhorse of LULCC modeling and has been widely implemented in different Geographic Information System (GIS) software packages (e.g. IDRISI, ArcGIS, Quantum GIS) or stand-alone applications (e.g. GEOMOD, CLUE-S, Dinamica EGO).

⁶ The software is freely available at <http://www.csr.ufmg.br/dinamica/>.

presenting transition rates P for all possible transitions between j LULC classes over one or multiple time steps expressed in v temporal units (ibid):

$$(1) \quad \begin{bmatrix} 1 \\ 2 \\ \vdots \\ j \end{bmatrix}_{t=v} = \begin{bmatrix} P_{11} & P_{12} & \dots & P_{1j} \\ P_{21} & P_{22} & \dots & P_{2j} \\ \vdots & \vdots & \ddots & \vdots \\ P_{j1} & P_{j2} & \dots & P_{jj} \end{bmatrix}^v * \begin{bmatrix} 1 \\ 2 \\ \vdots \\ j \end{bmatrix}_{t=0}$$

Within this system, the state of class 2, e.g. area change in class 2 at time v , depends on the sum of changes from class 2 to all other classes j expressed in percent of the initial stage of class 2 at $t=0$ during v . Once the transition rates P_{jj} have been calculated, the WoE method assesses the influence of a spatial variable on the spatial probability of a transition $i \rightarrow j$ independently from the effects of a combined solution. These spatial variables might represent certain (sets of) drivers or underlying causes. The conditional probability of transition D (e.g. deforestation) given a spatial variable C (e.g. distance to settlements) $P\{D|C\}$ can be expressed as (Follador et al. 2008):

$$(2) \quad P\{D|C\} = \frac{P\{D \cap C\}}{P\{C\}} = P\{D\} \frac{P\{C|D\}}{P\{C\}}$$

Equation 2 can be transformed into logits, where W^+ is the Weights of Evidence of occurring a deforestation event D given a spatial pattern C (B. S. Soares-Filho, Rodrigues, and Costa 2013):

$$(3) \quad \log\{D|C\} = \log\{D\} + W^+$$

This approach can be extended to relate a transition to several spatial variables, environmental criteria or patterns C_n to estimate the spatial post-probability of the transition D :

$$(4) \quad P\{D|C_1 \cap C_2 \cap C_3 \cap \dots \cap C_n\} = \frac{e^{\sum W_n^+}}{1 + e^{\sum W_n^+}}$$

where C_n are the values of n spatial variables observed at location x, y and represented by their specific Weights of Evidence W_n^+ . Since WoE only applies to categorical data, continuous data has to be categorized preserving the data structure (B. S. Soares-Filho, Rodrigues, and Costa 2013). The WoE method generates a Probability map of LULC transitions which can be used to predict future transitions based on additional rules or criteria.

The choice of the modeling approach depends on the targeted scale and availability of data. To bypass the restrictions imposed by data availability, land-use modelers tend to incorporate the drivers (and underlying causes) indirectly by choosing suitable proxies, e.g. spatially explicit features (road networks, settlement patterns) representing biophysical, political, or socioeconomic drivers. The WoE approach is particularly useful to assess the influence of these proxies on the observed deforestation pattern using spatial proxies.

1.3 Available data sets

The 1990-2000-2007-2010 deforestation on Santo Island is based on three types of data sets. Remote sensing data and results covering different periods have been used to reconstruct the deforestation trajectory for the periods 1990-2000, 2000-2007, and 2007-2010. The National Census of Population and Housing data and the Agricultural Census data published by Vanuatu's National Statistics Office served as a basis to conclude which drivers and underlying causes have to be considered in projecting the future deforestation trajectory. Thirdly, data providing the location of settlements, roads, and landscape features are required to develop the driver proxies. The following sections briefly discuss the potential and limitations of the different data sets.

1.3.1 Data providing the historic deforestation patterns

Three remote sensing data products were considered in this analysis:

Period 1990-2000: Vanuatu counts with a wall-to-wall deforestation assessment covering the period 1990 – 2000. The assessment developed a specific method based on indices combined in

pseudo spectral channels, applied it to high-resolution data (1990: Spot 1 /2 and Landsat 4, 2000: Landsat 7, Aster) and detected deforestation patterns at a minimum mapping unit (MMU) of 0.3ha (Herold et al. 2007). The study reports a gross deforestation for all islands between 1990 and 2000 of 4.677,6 ha or 467.8 ha/year, with more than 1/5 of the total forest loss observed on Santo Island (ibid.). Three land cover categories based on tree canopy cover density (bare area: less than 10%; woodland: 10-40%; forest: more than 40%) were detected. The results include a 2000 forest/non-forest cover map and a 1990-2000 deforestation map. The GIS data delivered to Vanuatu's Department of Forestry (DoF) indicates that the Santo's annual deforestation rate reached 970 ha or 97 ha/year (see Table 3, page 28).

Due to lack of suitable reference data covering the past, the geometric and thematic accuracy of the product is unknown. Some issues reduce its potential for establishing consistent long-term time-series of deforestation rates and patterns. First, it remains unclear, whether the deforestation product has been processed applying a forest definition related to the highest density class (more than 40% tree cover). The report does not state that explicitly. The metadata of the deforestation product refers to class 3 as "land forest loss". Secondly, the deforestation product and the 2000 forest/non-forest cover map do not match. Overlaying both coverages reveals that 1990-2000 deforestation patterns intersect with 2000 woodlands and forest (!) cover. The report suggests that the 2000 forest/non-forest cover map has been processed, first to be used as a baseline for the change detection. In any event, change patterns should be consistent with the final time stamp. A third limitation relates to the use of Spot data for the year 1990. The change detection method uses the Normalized Difference Water Index, which requires a short-wave infrared band as an input. While Landsat 4/5/7 and ASTER cover this spectrum, the HRV-2 instrument of early SPOT 1-3 satellites did not. Thus, it remains unclear, how the SPOT data had been processed.

Period 2007-2010: This period has been covered processing ALOS Palsar fine beam dual polarization (FBD) L-band Synthetic Aperture Radar (SAR) data to detect land cover change patterns (Mendez Zeballos and Seifert-Granzin 2013) applying methods developed by JAXA, the Japan Aerospace Exploration Agency (Isoguchi 2012). The initial analysis (Mendez Zeballos and Seifert-Granzin 2013) did not count with the Palsar scene S14E167 covering the northeastern part of Santo. For the development of the deforestation assessment, the missing scene has been procured and processed. The updated processing indicates a gross deforestation of 854.7 ha or 284.9 ha/year⁷ for Santo Island.

Although a very-high resolution coverage of Santo for 2011 (WorldView-2) is available, the accuracy of the SAR based change detection product can't be assessed. Assessing the accuracy of change patterns requires independent reference for the geometric and thematic accuracy of the product describing the initial state (here land cover 2007) and the final state (Fichet et al. 2013). Visual comparison between the SAR derived change patterns with the VHR data reveals that a substantial part of the change has been detected in and around agricultural lands suggesting that the algorithm accounts for seasonal changes in agricultural patterns. Avoiding such an overestimation would require a consistent forest/non-forest cover representing the baseline for the initial state, which is so far not available.

Period 2000-2007: To close the gap between the two periods, the 2000 – 2012 global deforestation data set recently published by the University of Maryland (Hansen et al. 2013) in cooperation with Google⁸ has been tested. For the period under consideration, a national forest cover loss of 1,755ha is being reported. Extracting the loss pattern for Santo indicates a tree cover loss of 82.6 ha for the same period. The global results are based on "tree cover" defined as all

⁷ This rate is still based on the number pixels. No filter to account for the MMU has been applied so far, to maintain consistency with the geometric resolution of the products, which report on a pixel basis.

⁸ The data is available at: <http://earthenginepartners.appspot.com/science-2013-global-forest/download.html>

vegetation taller than 5 meters in height. The global product provides a year 2000 tree coverage in percent as a baseline for calculating the change between 2000 and 2012. Then, the detected change is being allocated to the years in-between the period using spectral metrics (ibid). An MMU is not explicitly reported. All results are based on the geometric resolution of raw Landsat 7 data (28.5m).

Using a consistent tree cover loss coverage for a longer period providing even annual change patterns can provide valuable insights in spatiotemporal LUC dynamics. Particularly, it would help to assess the performance of certain deforestation drivers. However, the product makes it difficult to anticipate a national forest definition⁹ to be applied consistently over multiple periods as requested by the modalities for National Forest Monitoring Systems established by the Warsaw Framework for REDD-plus¹⁰.

This review of the applied remote sensing data products reveals that it is currently not possible to base the deforestation baseline on consistent time series of detected deforestation patterns. Additional processing is required to consolidate the input data. Section 4 provides recommendations how to proceed.

1.3.2 Socio-economic data

Over the last four decades, the Government of Vanuatu conducted several national censuses on population and housing (1967, 1979, 1989, 1999, 2009). Data of the last census aggregated at the province level has been published (Vanuatu National Statistics Office 2009b; Vanuatu National Statistics Office 2009a). The report provides data for the selected urban centers (Luganville, Port Vila) and provinces. Data for the Sanma province can be used as a proxy for Santo Island, as the province includes only Santo, the smaller island Malo, and a few very small islands. In case of demographics, the 2009 report provides data capturing the long-term past and future dynamics of demographic growth. Apart, Vanuatu conducted a few agricultural censuses. The last report dates from 2007 (Vanuatu National Statistics Office 2008) and refers to early agricultural census activities conducted in 1991, 1992, and 1993. While the Agricultural census provides valuable insights regarding the contribution of common livestock systems and agricultural practices to the livelihood of households it does not provide data to build time series reflecting the dynamics of changing land use.

1.3.3 Other data on spatial proxies

To capture the influence of spatial proxies, such as settlement patterns, road networks, distance to market access, GIS data of the Vanuatu Resource Information System (VANRIS) has been processed (Bellamy 1993). Biophysical parameters (slope, altitude) were derived from the TopoSAR Digital Surface Model (DSM) procured by the Department of Agriculture.

The following section describes how the data has been used in the processing chain.

2 Projecting future deforestation using Dinamica EGO

2.1 Overview on the processing chain

The following processing chains build on the land-use and land-cover change simulation model developed by B. S. Soares-Filho, Rodrigues, and Costa (2013). It has been implemented in version 2.4, the latest Dinamica EGO release. All input and modeling files are stored in the folder c:\Dinamica_VAN. Using the same folder structure is a precondition to run the models on other computers.

⁹ A national definition based on a percent-tree-cover threshold could be applied to derive a modified forest/non-forest cover for the 2000 baseline map. However, the amount of detected 2000-2012 tree cover loss can't be modified by the user.

¹⁰ The Decision 11/CP.19, par. 3 (FCCC/CP/2013/10/Add.1) requests that data and information should be "transparent, consistent over time, and suitable [for MRV]".

The model consists of a series of processing steps going from data preparation (calculating transition matrices, calculating ranges to categorize continuous data), to the assessment of WoEs (calculate weights of evidence, analyze map correlation), to the calibration of the simulation (set-up and run LUC simulation model, validate model, re-run simulation, project deforestation trajectories). Model adjustments are explained in each processing step. While these steps could be integrated into one simulation model, it is recommended to keep them apart to reduce processing time and allow for adjustments. The folder c:\Dinamica_VAN\Models stores all processing steps including sub-routines. Running the models requires a basic knowledge of Dinamica EGO, which can be gained passing through the tutorial¹¹.

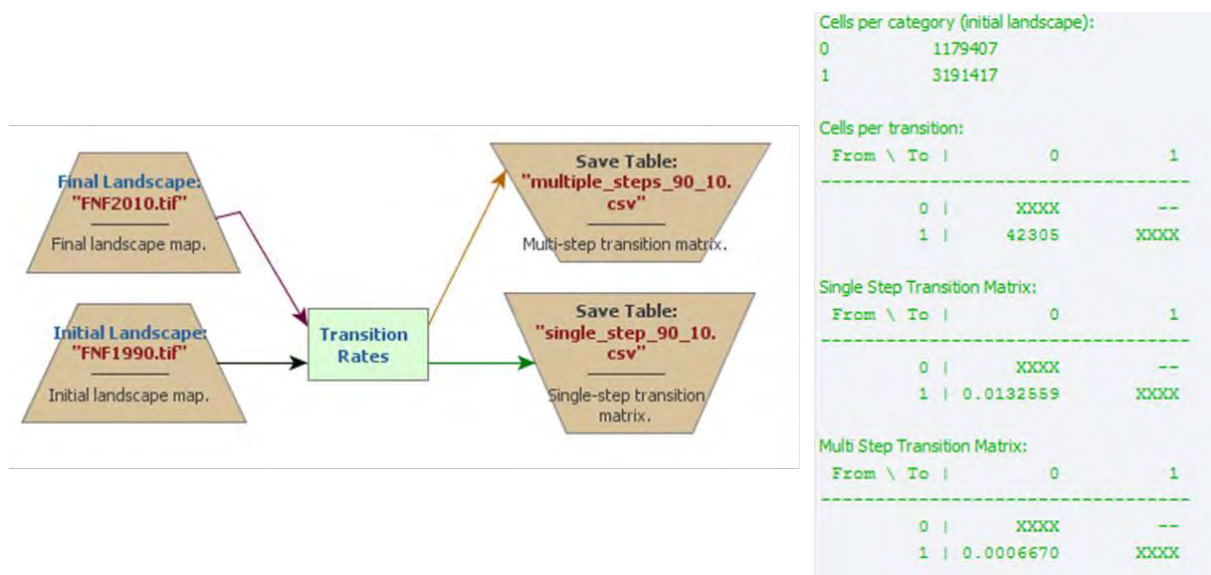
2.2 Processing steps

Step 1: Calculating the transition matrix

All input data needs to be of the same size in terms of cell size, cell number, projection, and extent. It is recommended to pre-process all the data in an external GIS, although Dinamica EGO provides some advanced map algebra functions, too. ArcGIS allows configuring the geo-processing environment, such that Arc Tool generates standardized outputs¹².

The inconsistencies between the three deforestation products (cf. section 2.1, p. 9) require adjustments leading to a de facto reduction of the reported deforestation rates. As the 1990-2000 change pattern does not match the 2000 forest mask, the forest/non-forest (FNF) map 2000 had to be used as the common reference to reconstruct the 1990 FNF cover by subtracting the 1990-2000 change from the 2000 forest map. Using the FNF 2000 cover as reference excludes all change signals of the following periods (2000-2007, 2007-2009), which appear outside the 2000 forest boundary. Consequently, the rates derived for the individual periods (cf. Annex 1) appear lower than the reported results in section 2.1).

Figure 2: Model and results of the transition matrix for the period 1990-2010



Dinamica EGO provides a function (a so called “functor”) to calculate the transition matrix based on standardized map inputs. Figure 2 shows the simple model (time steps = 20) and the resulting transition matrix (cf. Equ.1, p.9). Due to the high uncertainties regarding the true level of the deforestation rate in each period, we opted for calculating the transition matrix for one single period, which is 1990 - 2010. Annex 1 provides the transition matrices for all possible periods. The matrix indicated, that the rate for the transition

¹¹ <http://csr.ufmg.br/dinamica/dokuwiki/doku.php?id=tutorial:start>.

¹² Set the processing extent and Snap raster source in Arc Map (Geoprocessing -> Environments -> Processing Extent) to the baseline file, for example the forest/non-forest map of the initial time step.

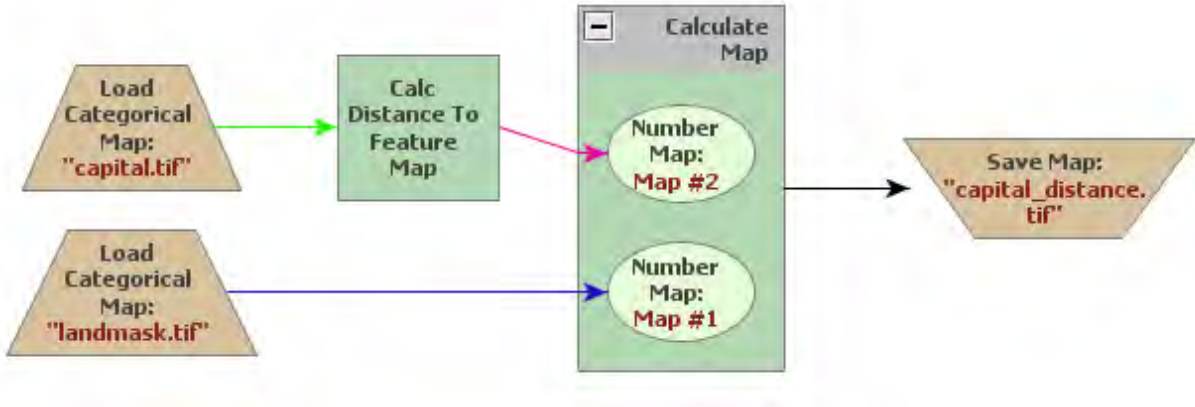
from class 1 (“forest”) to class 2 (“non-forest”), i.e. the gross deforestation rate reaches 1.32559 % reflecting a change of 42,305 cells or 3,807ha¹³. The annual deforestation rate reached 0.0667 %.

Step 2: Calculating ranges to categorize continuous data

The weights of evidence analysis of drivers requires an initial hypothesis which proxies deemed suitable to represent certain spatial constellations of drivers and underlying causes which can’t be assessed, directly. Table 3 introduced the proxies and related assumptions regarding the link between proxy and driver/causes selected for Santo Island. Driver proxy maps have been derived from the VANRIS database and the new TopoSAR based topographic map.

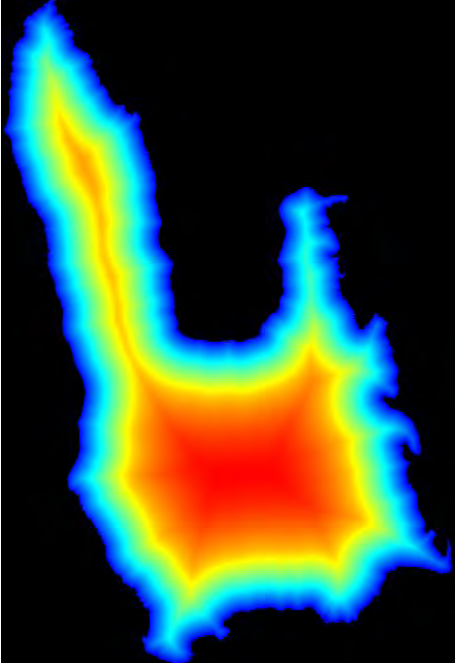
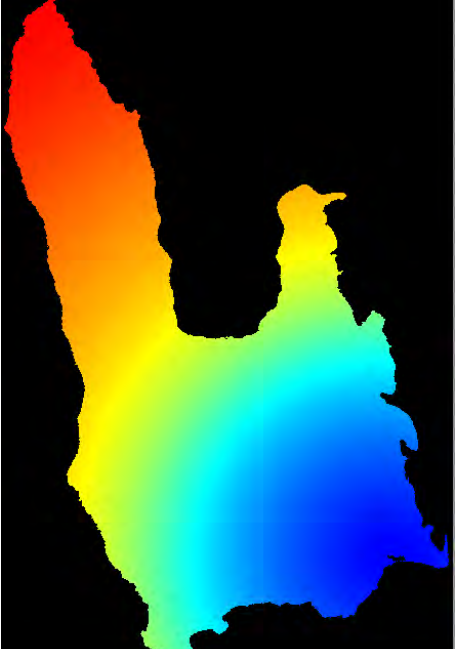
All vector data has been converted to 30m Geotiffs, fit to one common processing domain, and exported to the ERS file format. As distance to transport routes and settlements is being considered a potential driver proxy, Euclidian distances to geographic features (coastline, roads, places, and capital) were calculated using Dinamica EGO’s *Calculate Distance to Feature Map* functor. To limit the valid domain of the distance maps to the land surface a land mask was applied in processing distance maps¹⁴. Figure 3 illustrates the procedure for the distance-to-capital map.

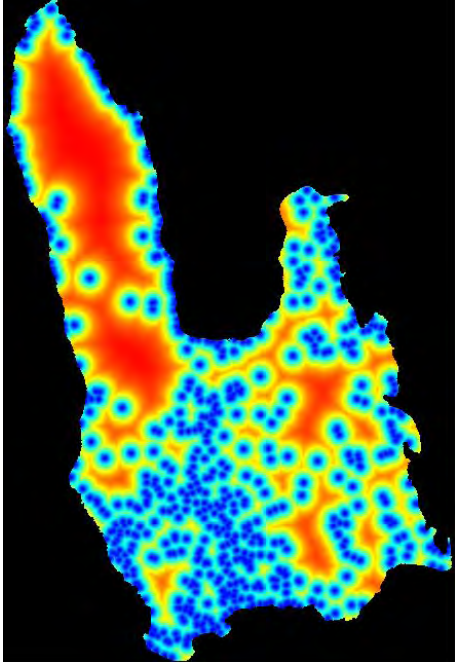
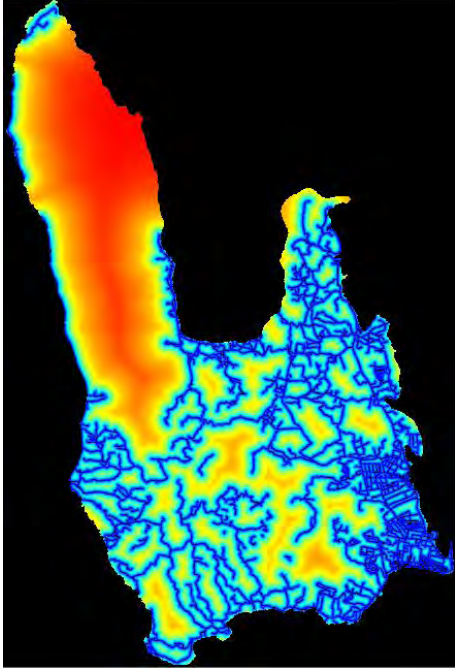
Figure 3: Distance map processing applied to the provincial capital

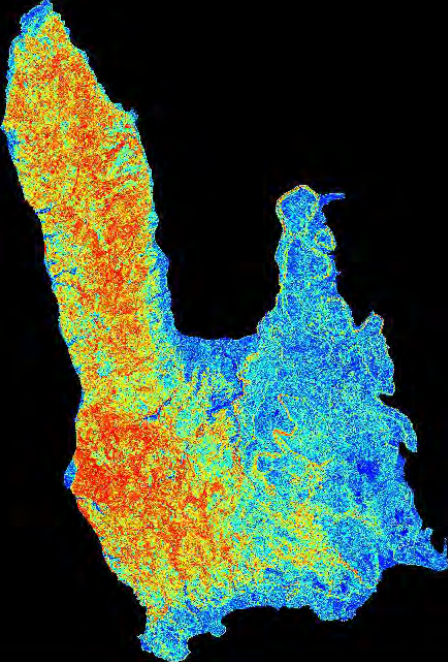



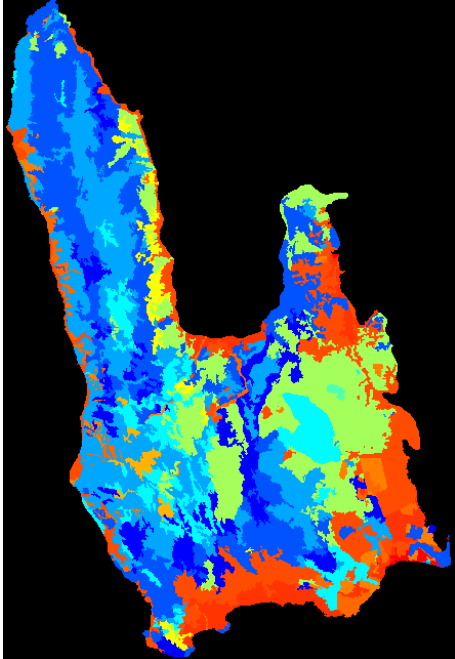
¹³ All input data were resampled to 30m geometric resolution.
¹⁴ The Calculate Map functor applies a simple map algebra equation which multiplies the resulting distance map with the land mask (raster value of land = 1, all other cells 0).

Table 1: Proxies and related drivers/causes

Proxy	Related drivers / causes	Assumptions
<p>Coastline</p> 	<p>Wood extraction</p> <ul style="list-style-type: none"> • Logging • Fuel wood • Charcoal production • Pole wood production 	<p>Proximity criteria: the coastline provides access to forests and resources extraction.</p>
<p>Distance to Luganville</p> 	<p>Wood extraction</p> <ul style="list-style-type: none"> • Commercial logging • Fuel wood • Charcoal production • Pole wood production <p>Agricultural expansion</p> <ul style="list-style-type: none"> • Economic: distance to national markets • Permanent cultivation • Demographic 	<p>Proximity criteria: Distance to the place with the highest population density and regional market drives demand for agricultural goods and timber.</p>

Proxy	Related drivers / causes	Assumptions
<p data-bbox="188 226 405 253">Distance to villages</p> 	<p data-bbox="675 349 850 376">Wood extraction</p> <ul data-bbox="675 398 925 524" style="list-style-type: none"> • Timber • Fuel wood • Charcoal production <p data-bbox="675 589 919 616">Agricultural expansion</p> <ul data-bbox="675 638 932 808" style="list-style-type: none"> • Livestock • Slash and burn • Crop production • Demographic growth 	<p data-bbox="1038 506 1406 651">Proximity criteria: Distance to the villages drives slash and burn practices, and demand for agricultural goods, fuel wood, charcoal, and pole wood</p>
<p data-bbox="188 954 379 981">Distance to roads</p> 	<p data-bbox="675 1245 935 1272">Infrastructure extension</p> <ul data-bbox="675 1294 836 1368" style="list-style-type: none"> • Transport • settlements 	<p data-bbox="1038 1249 1433 1368">Proximity criteria: Roads facilitate access to forests, forest conversion, and the development of new settlements.</p>

Proxy	Related drivers / causes	Assumptions
<p>Slope</p> 	<p>Wood extraction</p> <ul style="list-style-type: none"> • Commercial logging <p>Agricultural expansion</p> <ul style="list-style-type: none"> • Slash and burn • Permanent cultivation 	<p>Topographic criteria: Slope might impede access to timber resources and subsequent conversion of logged forest to agriculture. Flat areas are more suitable for agriculture.</p>
<p>Distance to non-forest edge</p> 	<p>Agricultural expansion</p> <ul style="list-style-type: none"> • Slash and burn • Permanent cultivation 	<p>Proximity criteria: the selection of sites to be deforested follows to a certain extend past deforestation practices.</p>

Proxy	Related drivers / causes	Assumptions
<p data-bbox="188 226 368 253">Vegetation cover</p> 	<p data-bbox="673 539 919 566">Agricultural expansion</p> <ul data-bbox="673 589 943 616" style="list-style-type: none"> <li data-bbox="673 589 943 616">• Permanent cultivation 	<p data-bbox="1040 533 1426 622">Vegetation can be used as a proxy for favorable climate conditions for agriculture.</p>

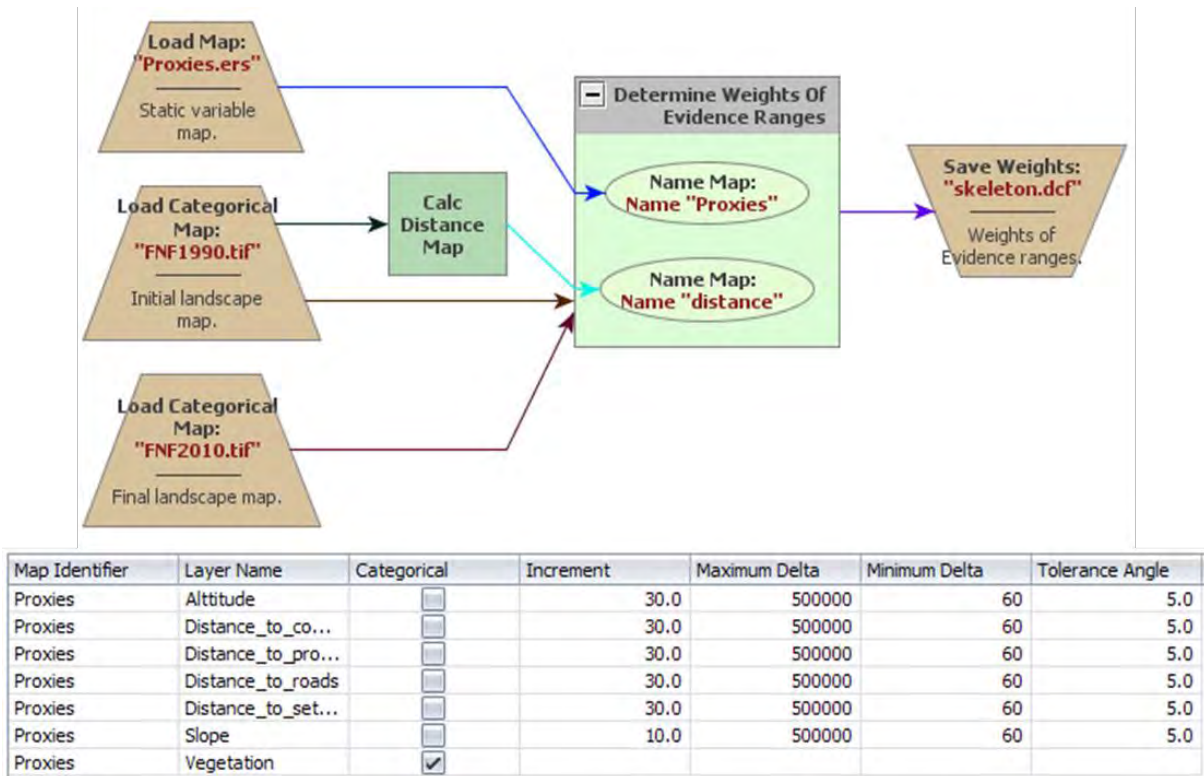
All proxy maps were stacked into one ERS-file using the *Create Cube* functor. The corresponding model *Cube.egoml* is available in the folder c:\Dinamica_VAN\Models\2_categorize_data.

Apart from the static driver maps listed in Table 3, the annually changing distance to forest edge has been included as a dynamic layer to be updated during every time step (cf. Figure 4). The dynamic layer anticipates the observations that deforestation activities follow past deforestation events to a certain extent creating so called fishbone patterns. Consequently, the forest edge of the former period could be considered a driver for subsequent deforestation activities, which is being captured iteratively by updating the distance-to-nonforest map. Thus, *Calculate Distance Map* has to be configured setting the category to which distance is being updated to 1 (= forest).

To assess the explanatory power of proxies for selected drivers and underlying causes, spatial input data has to be transformed into categorical data. All proxies expressed as continuous values have to be transformed into categorical maps using the *Determine the Weights of Evidence Ranges* Functor. Here, all distance maps have been transformed using a standard increment of 30 (besides the slope's increment to be set to 10 due to its limited parameter range), a minimum delta of 60, a maximum delta of 500,000 and a tolerance angle of 5.0 in configuring the categorical transformer within the function determining the weights of evidence ranges (figure 4).

The output of this step is the skeleton file providing the transformed potential categorical proxy ranges. At this stage, the ranges have been derived from the statistical properties of proxy maps themselves and do not show any explanatory power.

Figure 4: Configuration of the Determine the Weights of Evidence Ranges Functor

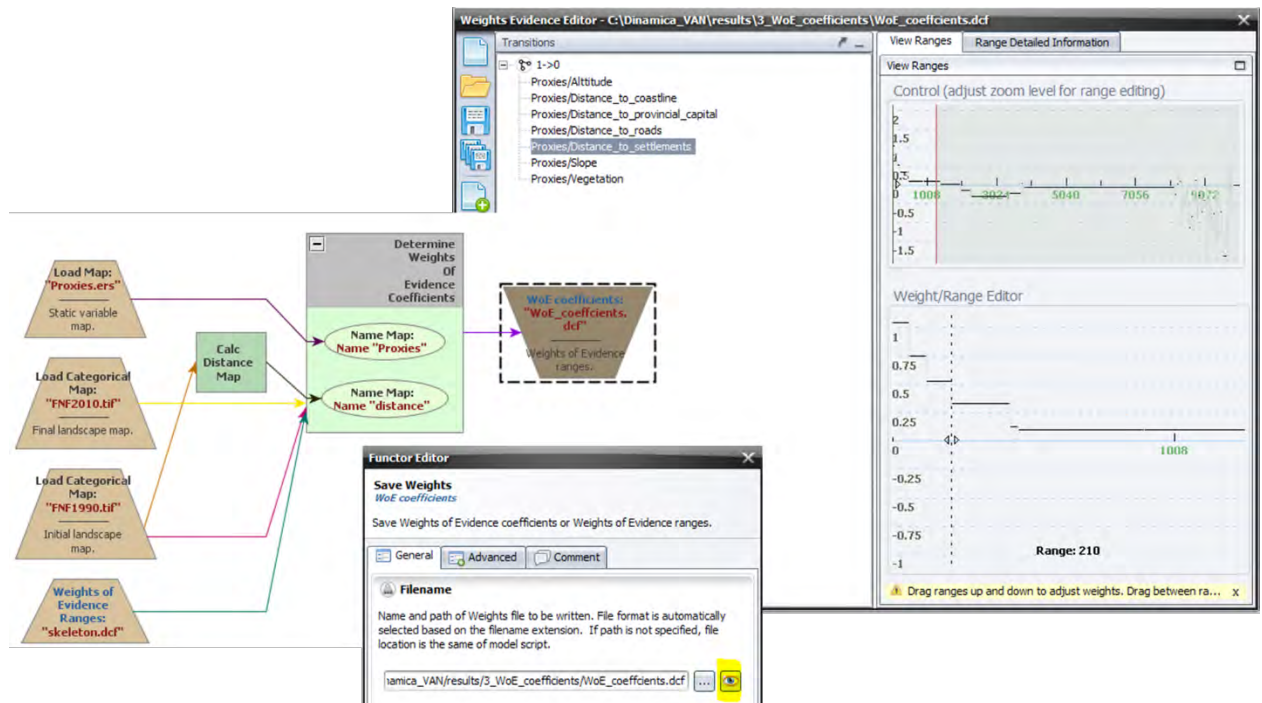


Within the next step, these ranges are linked to the observed patterns to derive coefficients, which qualify the range intervals in terms of their explanatory power regarding the forest cover change pattern.

Step 3: Calculating WoE coefficients

Once the ranges of the categorical proxies have been determined, the model of step 2 has to be re-run using the weights skeleton as an input. The model determines a functional relationship between a parameter representing a certain proxy range and its explanatory power regarding the observed pattern. Dinamica EGO provides a viewer (cf. Figure 5) visualizing the functional relation between the range of the variable and its explanatory power. A positive coefficient value indicates that the proxy actually “drives” the observed change within this range, values closed to 0 flag that there’s no relationship between the proxy and the change in the given range. Negative values indicate, that the relationship is averse for a given range, in the sense that the proxy contributes to avoiding land-use change. The numerical results are stored in a WoE coefficient file. The Excel-file stored in the corresponding results folder provides its content in a more readable format. The example in figure 5 indicates, that distance to road is only significant in explaining observed deforestation patterns up to a distance of 210 meters from the center point of the settlement. Evidently, the significance of the proxy range depends on the quantity of deforestation, the thematic accuracy of the FNF maps, and the positional accuracy of the proxy.

Figure 5: Visual interpretation of the significance of WoE coefficients



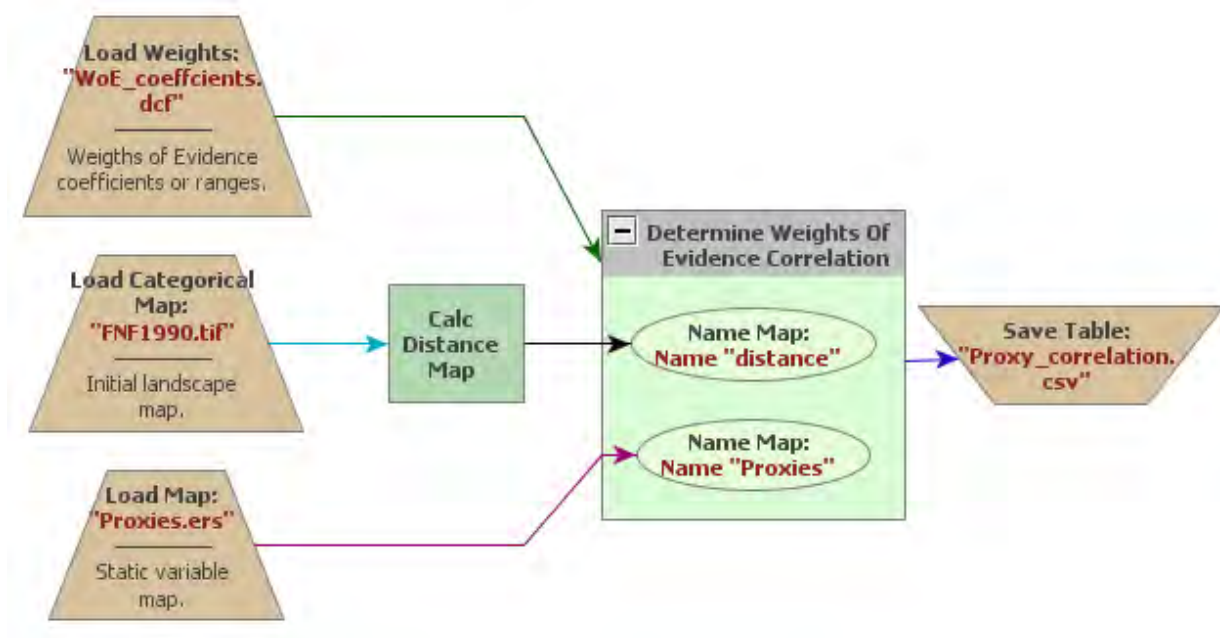
Results indicate that altitude has a limited explanatory power. Distance to the coastline is significant for deforestation up to a distance of 210m, while distance to Luganville could explain deforestation patterns up to a distance of 12 km. In case of roads, the critical threshold is 90m due to the denser road network around Luganville. Beyond 40 degrees, slope becomes a significant proxy as only a limited amount of deforestation doesn't occur on steeper slopes. The vegetation map provides a self-fulfilling prophecy, as the most significant classes appear to be Grasslands (classes 10 and 11).

Step 4: Analyzing map correlation

The eventual correlation between proxies has to be assessed pairwise to verify the requirement that the spatial variables have to be independent. Dinamica EGO provides a function ("Determine Weights of Evidence Correlations") calculating different correlation measures for all possible proxy pairs. Annex 2 provides the results of the assessment, as included in the file proxy_correlation.csv.

Although there is no agreed procedure how to compare the correlations measured by different statistical concepts, the pairs with the highest correlation in each indicator are candidates to be ruled out. Here, the pairs "altitude" / "vegetation" and "Distance_to_provincial_capital" / "Distance_to_roads" reach the highest correlation in both indicator groups, while other pairs don't appear to be correlated (Annex 2). Consequently, one of the two proxies within each pair has to be ruled out. As altitude shows little explanatory power it is a good candidate. Distance to roads is excluded as well, as the density of the road network limits the predictive power due its limited distance ranges. To anticipate these modification the WoE_coefficients.dcf file has to be edited within the model and stored under a new name (WoE_coefficients_wo_correlations.dcf).

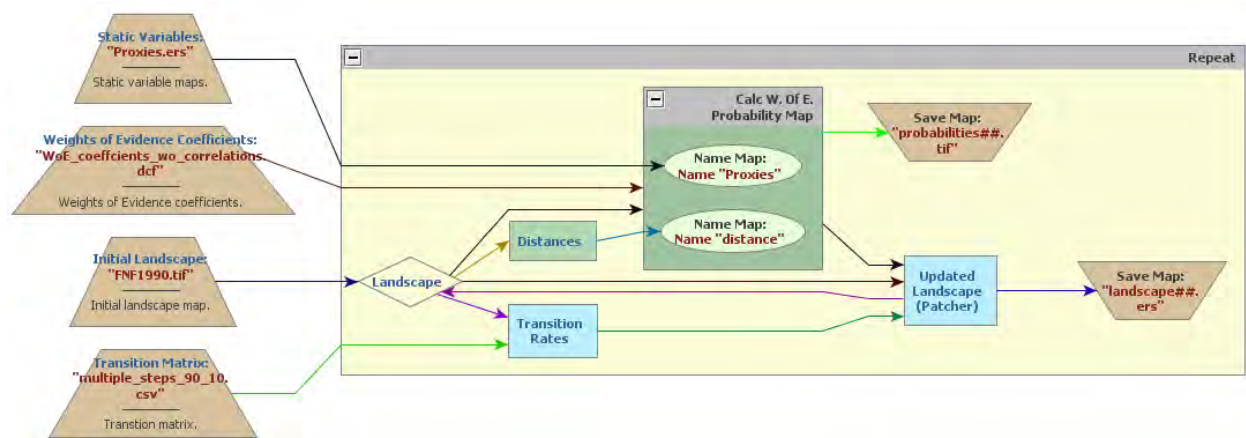
Figure 6: Configuration of the correlation assessment model



Step 5: Simulating LULC change for the period 1990 - 2000

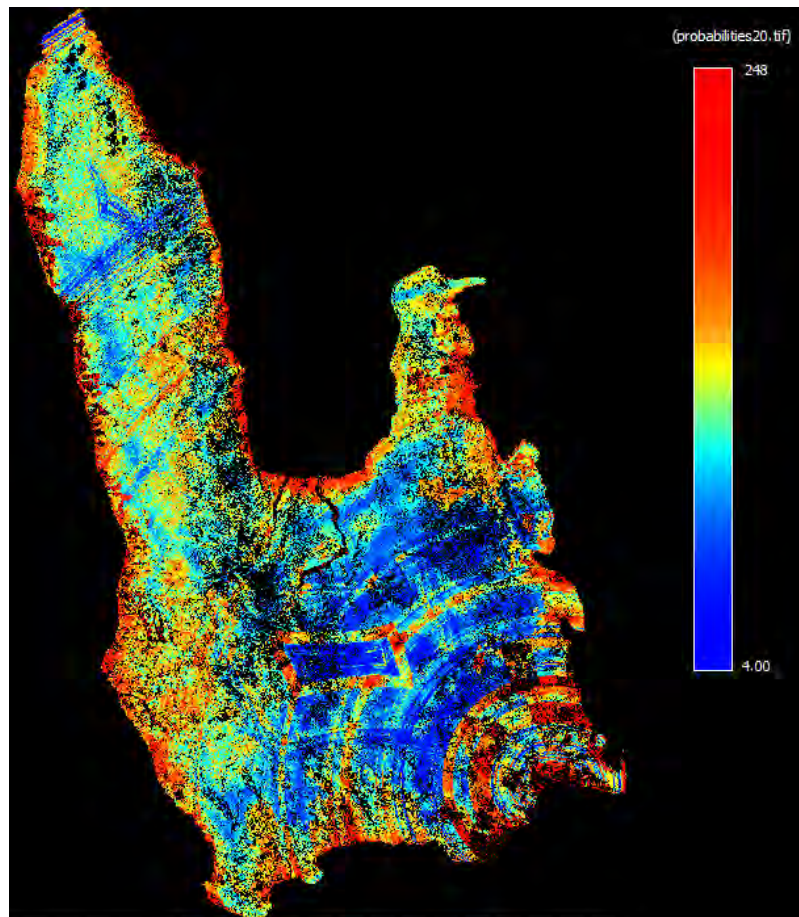
The configuration of the simulation model requires several new functors and, of course, the calibration files (WoE coefficients, multiple step transition matrix). The tutorial (B. S. Soares-Filho, Rodrigues, and Costa 2013) and the internal Help function explain the different functors in detail. The model runs 20 time steps generating annual FNF maps (landscape##.ers with ## = time step) and probability maps. In its current configuration, it doesn't allow for the formation of random forest patches through a seeding mechanism (all *Patcher* parameter set to 1.0). This restriction can be relaxed in complementary runs depending on the type of observed deforestation pattern. The complementary functor *Expander* expands existing deforestation patches leading to fishbone patterns. Considering Santo's past deforestation patterns, the *Patcher* configuration deems more appropriate.

Figure 7: LULCC simulation model for the period 1990 - 2000



The resulting probability maps reveal that the distance to the provincial capital shows an overarching impact on the deforestation probability (figure 8).

Figure 8: Deforestation probability map for year 2010

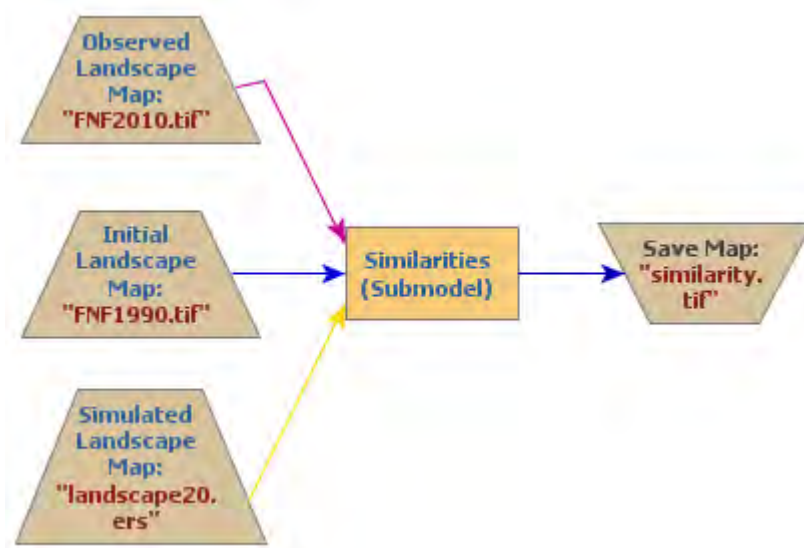


The resulting FNF map for time step 20 (landscape20.ers) can be compared with the detected FNF cover for year 2010.

Step 6: Validating the LULCC simulation

Dinamica EGO provides sophisticated functions to assess the similarity between observed and simulated spatial patterns. Considering the heterogeneity and deficiencies of the input data, we chose the default configuration (figure 9).

Figure 9: Similarity assessment for period 1990 - 2000

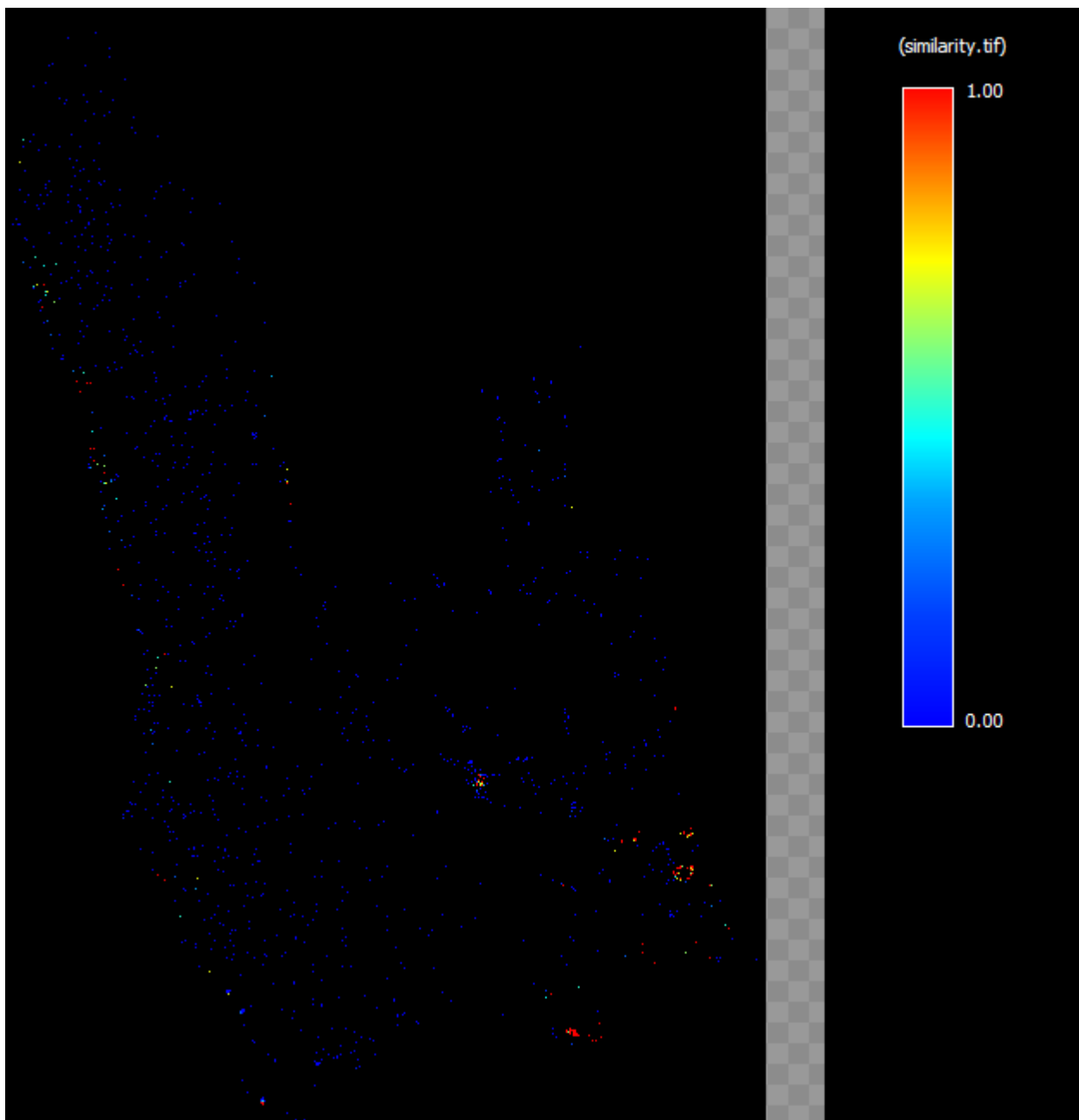


Not so surprisingly, the resulting similarity map reflects the scattered patchy deforestation pattern of the reference period. As figure 10 shows, similarity is pretty low. Good matches between observed and simulated patterns occur only close to settlements and the provincial capital. This relates to the generally low deforestation rate, compared to the overall forest cover. Furthermore, uncertainties regarding the true quantity, thematic and positional accuracy of land use change lead to noise, which reduces the explanatory power of the WoE coefficients and the predictive power of the model.

Step 7: Validating the LULCC simulation at multiple resolutions

Complementary to step 6, Dinamica EGO provides the option to conduct the similarity assessment at different resolutions under the assumption that part of the data inherent noise might be damped at coarser resolutions. The assessment reveals that no significant improvements can be achieved by shifting to lower spatial resolutions.

Figure 10: Similarity between simulated and observed deforestation for the period 1990 - 2000



Step 8: Simulating LULC change for 2010 - 2020

The weak similarity raises doubts whether sound correlations between socio-economic parameters and deforestation rates can be derived. Comparing deforestation rates against reported demographic growth indicates that the deforestation rate exceeded population growth during the last decade (cf. Table 2). As the deforestation rates themselves remain uncertain, robust correlations can't be achieved at this stage.

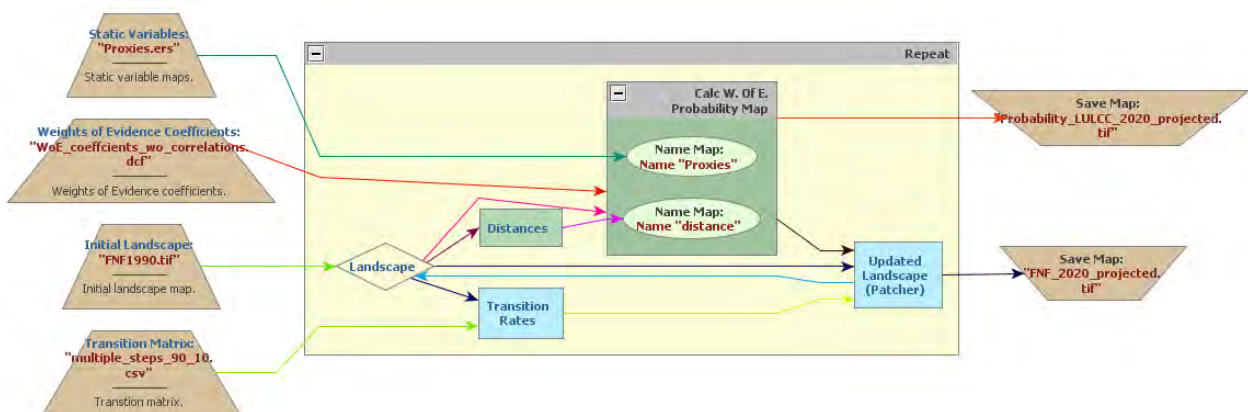
Table 2: Deforestation rates and demographic growth 1990 – 2010

	Population increment	Deforestation increment
	# inhabitants	# ha
1989-1999	10,542	970
1999-2009	9,771	2,838

Source: (Vanuatu National Statistics Office 2009a); own calculations

Thus, the simulation model developed in step 5 will be used in a conservative mode projecting deforestation patterns for 2010 to 2020 based on the detected rates for 1990 – 2000, setting the number of iterations to 30 (functor *Repeat*).

Figure 11: Deforestation projection model 1990 - 2020



To reduce storage, this model generates a probability map for the whole period (1990-2020) and the projected FNF map for the year 2020.

3 Discussion of results

Based on the WoE configuration for the period 1990-2010 and the corresponding average deforestation rate, the model projects a deforestation rate of 0.07% for the period 2011-2020. With 0.07%, the average annual deforestation rate remains low. Figure 12 indicates, that most of the deforestation will occur in the surroundings of the provincial capital and, to a lesser extent, along Santo's west coast.

Figure 12: Projected 2020 forest cover and 2011 – 2020 deforestation

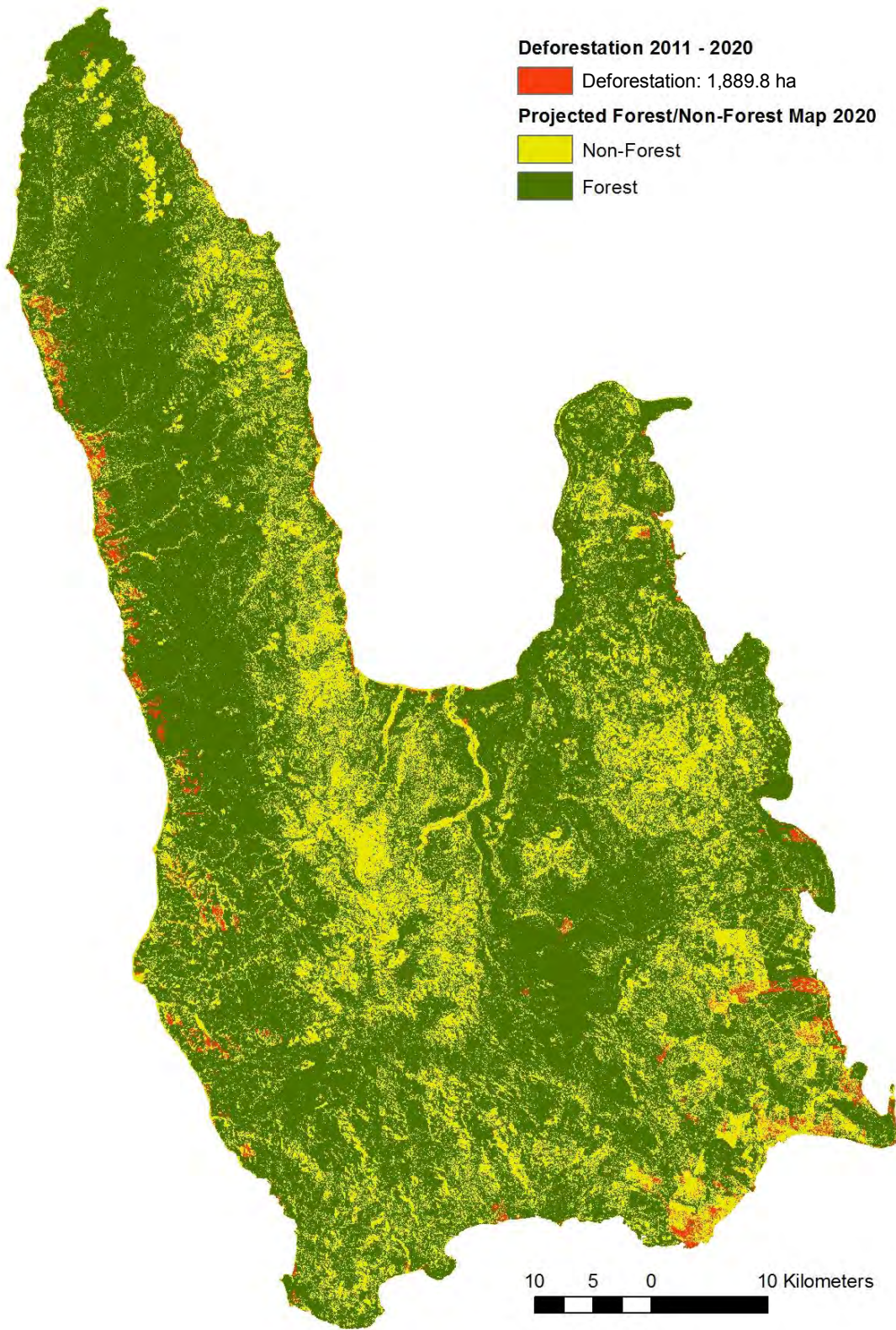
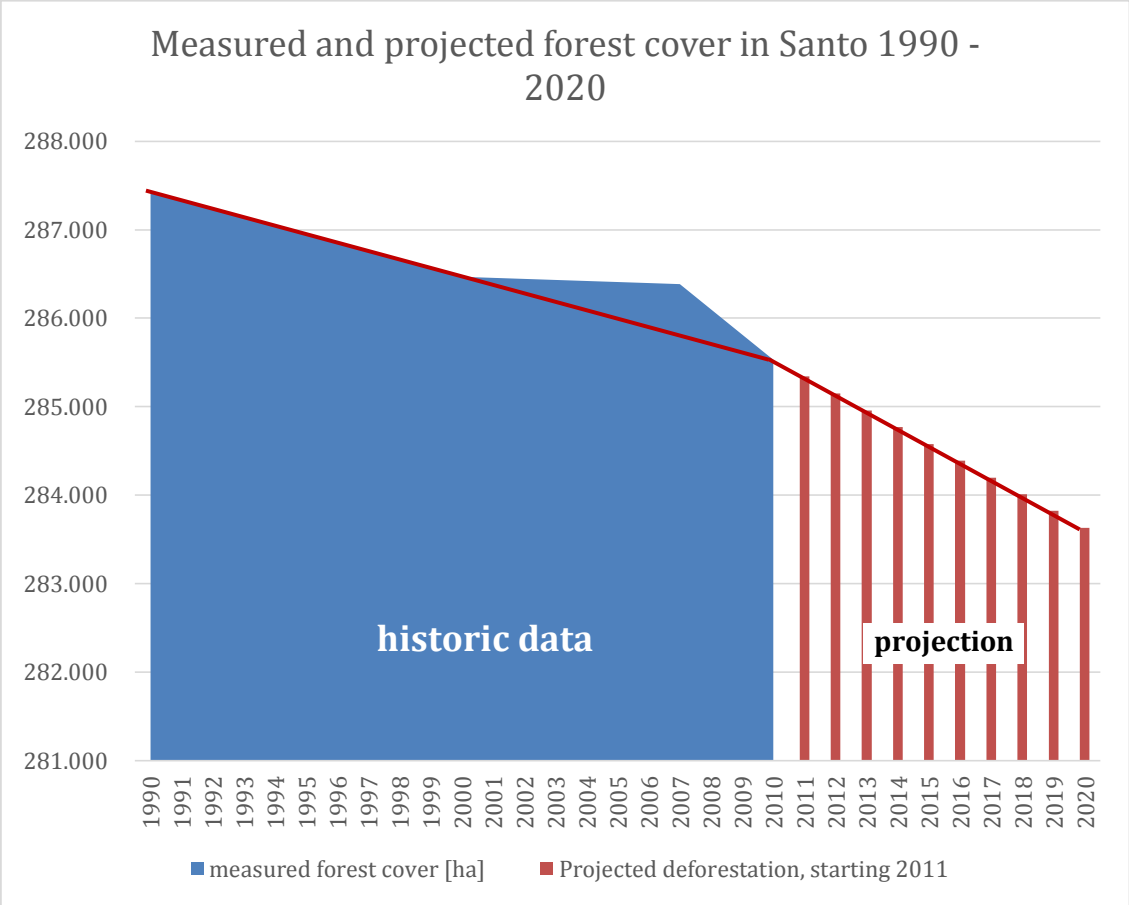


Figure 13: Historic and projected forest cover change on Espiritu Santo Island, 1990 – 2020



The graph in figure 13 shows the total forest cover on Espiritu Santo for each year between 1990 and 2020, divided into measured historic and projected forest coverage. With a projected annual 0.07 % deforestation rate, the predicted forest cover loss is twice as fast as in the 20 years before, even though it slows down significantly compared to the years 2007 – 2010. Table 3 below shows the measured and predicted deforestation in Santo in a comparison of area and rate for the observed time periods and on annual basis.

Table 3: Comparison of total and annual area; total and annual rate of deforestation in Santo Island for the observed and projected periods

Period	Total deforestation [ha]	Total deforestation rate	Annual deforestation [ha]	Annual deforestation rate
<i>1990-2000</i>	969.8	0.34 %	97	0.034%
<i>2000-2007</i>	82.6	0.03 %	11.8	0.004%
<i>2007-2010</i>	854.7	0.3 %	284.9	0.1%
<i>Total 1990 - 2010</i>	1907.1	0.33 %	95.4	0.033%
<i>2010-2020 (projected)</i>	1,898.8	0.67 %	189.9	0.067%

It is not fully clear why the deforestation between 2000 and 2007 dropped significantly in comparison to the earlier decade and especially to the following three years. While the data availability might be one reason, the trend is still obvious. An attempt to explain the difference is that the highest impact on the forests in Vanuatu is forest degradation. Highly degraded forest area will be quickly converted to non-forest land when a new economic opportunity turns up. In order to consolidate this analysis, economic production data for 2000 – 2010 should be analyzed to investigate a possible influence on the deforestation pattern.

Due to the explained limitations, the explanatory power of the WoE coefficients and the projective power of the LULCC model remains rather weak. Improving the quality of the inputs, particularly their thematic / geometric, and their positional accuracy, will not only improve the temporal consistency of the analysis, but provide more accurate results and improvements in model calibration.

4 Recommendations

4.1 Improvements of the change detection processing chains

The results of a simulation model can only be as reliable as its input data. High uncertainties regarding the historic deforestation rate and patterns limit the precision of the probabilistic weights-of-evidence assessment to quantify the impact of proxy drivers. This limitation affects the validity of the simulated future deforestation rate and pattern. While it is possible to develop the model further, for example by implementing sub-regions with specific transition rates and weight-of-evidence configurations, the first priority should be improving the consistency of the input data. To achieve this goal, the following steps, working backwards in time to achieve temporal consistency, are recommendable:

1. Instead of using the 2000 forest/non-forest map as a baseline for classifying past and future change patterns as deforestation, the processing shall be based on a validated forest / non-forest map with known accuracy. This requirement points to year 2010, for which VHR data is available to serve as an independent higher-resolution verification source. As optical data for this year is scarce, it is recommended to develop a SAR-based 2010 FNF cover applying JAXA's default methodologies¹⁵ to available ALOS PALSAR data. Although the accuracy of the product might be slightly lower than the one based on multispectral optical data, it will be almost cloud-free and consistent with the SAR-based change detection for the period 2007-2010.
2. The accuracy of the SAR-based 2007-2010 has to be assessed. Its verification requires at least one VHR coverage for the area around Luganville, showing the highest dynamics in LULC change. If a validated and verified 2010 FNF map is available it can be included in a modified processing chain as proposed by JAXA (JAXA 2012) to improve its thematic accuracy.
3. Covering the period 2000 – 2007 is the most challenging task. As there is very little suitable multispectral optical data available, options are limited. Vanuatu's default method for LULCC detection based on optical data can be used, but certain data gaps will remain due to cloud cover and the scan line correction error of Landsat 7. The reference image for verifying the SAR-derived 2007 FNF cover can be used as reference for the 2000 – 2007 change detection. Remaining gaps shall be mapped and could eventually be filled either by the 2007 FNF map or the 2000 FNF map (see next step).
4. The 1990-2000 deforestation assessment is key for capturing the long-term trend of certain deforestation drivers and for justifying that Vanuatu's deforestation baseline needs to be adjusted upwards. It is the opinion of the authors, that the 1990-2000 change detection has to be modified and reprocessed based on a forest definition to be consistently applied across all the processing periods. If the default method (Herold et al. 2007) is to be used, SPOT data must not be included as it doesn't provide the necessary short-wave infra-red band. This condition will limit the options to cover 1990 even more. The availability of almost cloud free Landsat TM4 data has to be assessed. If there is no alternative to SPOT, the change detection method has to be adjusted to the band characteristics.

¹⁵ As of now, JAXA considers two types methods: (JAXA 2012) provides shell scripts for image segmentation and classification. The classification scripts encompass various classifiers. Recently, JAXA is considering using the Remote Sensing and GIS Software Library (RSGISLib).

Our final recommendation relates to the current availability of Landsat 8 data covering Vanuatu's territory. As of now, Vanuatu's Landsat 8 coverage stays behind the acquisition frequency over continental areas. While continental areas were covered at around two scenes per month during the last 11 months, Vanuatu has been covered by 7 scenes only. It is of utmost importance for the sustainability of the National Forest Monitoring system, that the Government of Vanuatu requests USGS to cover the small island states in the same way as the continental areas.

4.2 Improvements of the modeling approach

Dinamica EGO offers several capabilities to be anticipated in a modeling approach building on consolidated data. Eventually, Santo can be divided into two sub-regions to be calibrated independently. While the deforestation pattern of Santo's west coast is framed by small scale agriculture and small-scale agricultural trade relying on shipping, land-use change in Santo's eastern part is driven by cattle ranching, medium scale agriculture, urbanization, and tourism development. Both differing dynamics can be accommodated in a regionalized model if suitable calibration data is available. However, model calibration can only start once the deforestation analysis has been consolidated.

4.3 Priorities for REL development

The deforestation baseline for Sanma province does not yet state the amount of carbon emitted from this activity. A forest carbon inventory will be implemented in the province in the third quarter of 2014, after which the carbon value will be added to the deforestation baseline to calculate a deforestation-related reference emission level.

Despite the difficulties in data accuracy, this study makes it clear that deforestation rates for Santo have been very low in the past and are expected to remain so in the near future. The Sanma province shares with the majority of Pacific Islands the fact that forest degradation is a much larger problem for sustainable resource management and greenhouse gas emissions. The potential for measures that sequester carbon is high. In the Pacific, countries should therefore focus on improving data and analysis on the impact of forest degradation on biomass and carbon contents in the region's forests. A baseline on historic and projected forest degradation must be the priority.

References

- Agarwal, C., G.M. Green, J.M. Grove, T.P. Evans, and C.M. Schweik. 2002. "A Review and Assessment of Land-Use Change Models: Dynamics of Space, Time, and Human Choice". U.S. Department of Agriculture, Forest Service, Northeastern Research Station, Newton Square, Pennsylvania, USA.
- Bellamy, Jennifer A. 1993. "Vanuatu Resource Information System. VANRIS Handbook". CSIRO Brisbane.
- Briassoulis, Helen. 2001. *Analysis of Land Use Change: Theoretical and Modeling Approaches*. The Web Book of Regional Science. Regional Research Institute, West Virginia University. <http://www.rri.wvu.edu/WebBook/Briassoulis/contents.htm>.
- Brown, Sandra, Myrna Hall, Ken Andrasko, Fernando Ruiz, Walter Marzoli, Gabriela Guerrero, Omar Masera, Aaron Dushku, Ben DeJong, and Joseph Cornell. 2006. "Baselines for Land-Use Change in the Tropics: Application to Avoided Deforestation Projects. Formal Report". <http://ies.lbl.gov/node/311>. <http://ies.lbl.gov/node/311>.
- Carlson, Kimberly M., Lisa M. Curran, Dessy Ratnasari, Alice M. Pittman, Britaldo S. Soares-Filho, Gregory P. Asner, Simon N. Trigg, David A. Gaveau, Deborah Lawrence, and Hermann O. Rodrigues. 2012. "Committed Carbon Emissions, Deforestation, and Community Land Conversion from Oil Palm Plantation Expansion in West Kalimantan, Indonesia." *Proceedings of the National Academy of Sciences* 109 (19): 7559–64. doi:10.1073/pnas.1200452109.
- Committee on Needs and Research Requirements for Land Change Modeling, Geographical Sciences Committee, Board on Earth Sciences and Resources, and Division on Earth and Life Studies. 2013. *Advancing Land Change Modeling: Opportunities and Research Requirements*. National Academy of Sciences. http://www.nap.edu/catalog.php?record_id=18385.
- Eggleston, H.S., L. Buendia, K. Miwa, T. Ngara, and K. Tanabe, eds. 2006. *2006 IPCC Guidelines for National Greenhouse Gas Inventories*. Vol. 4: Agriculture, Forestry, and Other Land Use. IGES, Japan.
- Fichet, Louis-Vincent, Christophe Sannier, Etienne Massard K. Makaga, and Frederique Seyler. 2013. "Assessing the Accuracy of Forest Cover Map for 1990, 2000 and 2010 at National Scale in Gabon." *IEEE Journal of Selected Topics in Applied Earth Observations and Remote Sensing*, 1–11. doi:10.1109/JSTARS.2013.2271845.
- Follador, M., N. Villa, M. Paegelow, F. Renno, and R. Bruno. 2008. "Tropical Deforestation Modelling: Comparative Analysis of Different Predictive Approaches. The Case Study of Peten, Guatemala." In *Modelling Environmental Dynamics*, edited by Martin Paegelow and María Teresa Camacho Olmedo, 77–107. Environmental Science and Engineering. Springer Berlin Heidelberg. http://link.springer.com/chapter/10.1007/978-3-540-68498-5_3.
- Geist, Helmut J., and Eric F. Lambin. 2001. "What Drives Tropical Deforestation? A Meta-Analysis of Proximate and Underlying Causes of Deforestation Based on Subnational Case Study Evidence." LUCC International Project Office.
- . 2002. "Proximate Causes and Underlying Driving Forces of Tropical Deforestation." *BioScience* 52 (2): 143. doi:10.1641/0006-3568(2002)052[0143:PCAUDF]2.0.CO;2.
- GOFC-GOLD. 2013. *A Sourcebook of Methods and Procedures for Monitoring and Reporting Anthropogenic Greenhouse Gas Emissions and Removals Caused by Deforestation, Gains and Losses of Carbon Stocks in Forests Remaining Forests, and Forestation*. GOFC-GOLD Report version COP19-1. Alberta, Canada: GOFC-GOLD Land Cover Project Office, Wageningen University, The Netherlands.

- Hall, C. A.S., H. Tian, Y. Qi, G. Pontius, J. Cornell, and J. Uhlig. 1995. "Modeling Spatial and Temporal Patterns of Tropical Land Use Change. *J. of Biogeography*, 22, 753-757." *Journal of Biogeography*, no. 22: 753–57.
- Hansen, M. C., P. V. Potapov, R. Moore, M. Hancher, S. A. Turubanova, A. Tyukavina, D. Thau, et al. 2013. "High-Resolution Global Maps of 21st-Century Forest Cover Change." *Science* 342 (6160): 850–53. doi:10.1126/science.1244693.
- Herold, Martin, Jacqueline Sambale, Martin Lindner, Marcel Urban, and Sean Weaver. 2007. "Satellite Based Monitoring of the National Forest Resources in the Pacific Island State of Vanuatu. Proceedings of the Tri-National Conference 2007 of the Swiss, Austrian and German Society for Photogrammetry and Remote Sensing, 19.-21.06.2007, Basel/ Switzerland, 319-328." In Von Der Medizintechnik Bis Zur Planetenforschung – Photogrammetrie Und Fernerkundung Für Das 21. Jahrhundert. Vorträge Dreiländertagung 27. Wissenschaftlich-Technische Jahrestagung Der DGPF 19. – 21. Juni 2007 in Muttentz, Basel. Vol. 16. Muttentz, Basel: Deutsche Gesellschaft für Photogrammetrie, Fernerkundung und Geoinformation e.V. DGFP.
- Isoguchi, Osamu. 2012. "Training of Forest Change Detection Using PALSAR Gamma Naught" November 5, RESTEC HQ Office.
- JAXA. 2012. "KC18 and JAXA-REDD+ Material Training Course on ALOS PALSAR Mosaic Analysis for Forest Monitoring."
- Leite, Christiane Cavalcante, Marcos Heil Costa, Britaldo Silveira Soares-Filho, and Letícia de Barros Viana Hissa. 2012. "Historical Land Use Change and Associated Carbon Emissions in Brazil from 1940 to 1995." *Global Biogeochemical Cycles* 26 (2): n/a–n/a. doi:10.1029/2011GB004133.
- Maeda, Eduardo Eiji, Barnaby J.F. Clark, Petri Pellikka, and Mika Siljander. 2010. "Modelling Agricultural Expansion in Kenya's Eastern Arc Mountains Biodiversity Hotspot." *Agricultural Systems* 103 (9): 609–20. doi:10.1016/j.agsy.2010.07.004.
- Mas, Jean-François, Melanie Kolb, Martin Paegelow, María Teresa Camacho Olmedo, and Thomas Houet. 2014. "Inductive Pattern-Based Land Use/covers Change Models: A Comparison of Four Software Packages." *Environmental Modelling & Software* 51 (January): 94–111. doi:10.1016/j.envsoft.2013.09.010.
- Mendez Zeballos, Dorys, and Jörg Seifert-Granzin. 2013. "SAR-Based Deforestation Assessment, Espiritu Santo Island, Vanuatu. Processing Description and Results Version 1.0."
- Meridian Institute. 2011a. "Modalities for REDD+ Reference Levels: Technical and Procedural Issues. Prepared for the Government of Norway, by Arild Angelsen, Doug Boucher, Sandra Brown, Valérie Merckx, Charlotte Streck, and Daniel Zarin." www.REDD-OAR.org.
- . 2011b. "Guidelines for REDD+ Reference Levels: Principles and Recommendations. Prepared for the Government of Norway, by Arild Angelsen, Doug Boucher, Sandra Brown, Valérie Merckx, Charlotte Streck, and Daniel Zarin." www.REDD-OAR.org.
- Penman, Jim, Michael Gytarsky, Taka Hiraishi, Thelma Krug, Dina Kruger, Riitta Pipatti, Leandro Buendia, et al. 2003. *Good Practice Guidance for Land Use, Land-Use Change and Forestry*. Hayama, Kanagawa, Japan: Published by the Institute for Global Environmental Strategies for the IPCC.
- Schaldach, Rüdiger, and Jörg A. Priess. 2008. "Integrated Models of the Land System: A Review of Modelling Approaches on the Regional to Global Scale." *Living Reviews in Landscape Research* 2 (1). <http://www.livingreviews.org/lrlr-2008-1>.
- Soares-Filho, B. S., H. O. Rodrigues, and W.L.S. Costa. 2013. *Modeling Environmental Dynamics with Dinamica EGO*. Revised Edition. <http://csr.ufmg.br/dinamica/dokuwiki/doku.php?id=tutorial:start>.

- Soares-Filho, Britaldo Silveira, Daniel Curtis Nepstad, Lisa M. Curran, Gustavo Coutinho Cerqueira, Ricardo Alexandrino Garcia, Claudia Azevedo Ramos, Eliane Voll, Alice McDonald, Paul Lefebvre, and Peter Schlesinger. 2006. "Modelling Conservation in the Amazon Basin." *Nature* 440 (7083): 520–23. doi:10.1038/nature04389.
- Thapa, Rajesh Bahadur, and Yuji Murayama. 2011. "Urban Growth Modeling of Kathmandu Metropolitan Region, Nepal." *Computers, Environment and Urban Systems* 35 (1): 25–34. doi:10.1016/j.compenvurbsys.2010.07.005.
- Turner II, B.L., David L. Skole, and William B. Meyer. 1994. "Global Land-Use/Land-Cover Change: Towards an Integrated Study Source." *Ambio* 23 (1): 91–95.
- Vanuatu National Statistics Office. 2008. "Census of Agriculture 2007 - Vanuatu."
- . 2009a. "2009 National Population and Housing Census. Basic Tables Report Volume 1."
- . 2009b. "2009 National Census of Population and Housing. Summary Release". Ministry of Finance and Economic Management.
- VCS. 2013. "Agriculture, Forestry and Other Land Use (AFOLU) Requirements. VCS Version 3 Requirements Document, v3.4."
- Verburg, Peter H., Paul P. Schot, Martin J. Dijst, and A. Veldkamp. 2004. "Land Use Change Modelling: Current Practice and Research Priorities." *GeoJournal* 61 (4): 309–24. doi:10.1007/s10708-004-4946-y.
- Walker, Wayne S., Claudia M. Stickler, Josef M. Kellndorfer, Katie M. Kirsch, and Daniel C. Nepstad. 2010. "Large-Area Classification and Mapping of Forest and Land Cover in the Brazilian Amazon: A Comparative Analysis of ALOS/PALSAR and Landsat Data Sources." *IEEE Journal of Selected Topics in Applied Earth Observations and Remote Sensing* 3 (4): 594–604. doi:10.1109/JSTARS.2010.2076398.
- Yi, Wei, Zhiqiang Gao, Zhihua Li, and Maosi Chen. 2012. "Land-Use and Land-Cover Sceneries in China: An Application of Dinamica EGO Model." In , edited by Wei Gao, Thomas J. Jackson, Jinnian Wang, and Ni-Bin Chang, 85130I–85130I–7. doi:10.1117/12.927782. <http://proceedings.spiedigitallibrary.org/proceeding.aspx?articleid=1382202>.

Annex 1: Transition matrices for different deforestation periods

	1990 - 2000		2000-2007		2007-2010		1990-2010		2000-2010	
Cells per category (initial landscape):										
0	1,185,512		1,196,288		1191099		1179407		1190182	
1	3,193,750		3,182,974		3179725		3191417		3180642	
Cells per transition	0	1	0	1	0	1	0	1	0	1
0		0								
1	10776		918		30613		42305		31530	
Single Step Transition Matrix:	0	1	0	1	0	1	0	1	0	1
0		0								
1	0.0033741		0.0002884		0.0096276		0.0132559		0.0099131	
Multi Step Transition Matrix	0	1	0	1	0	1	0	1	0	1
0		0								
1	0.0003379		0.0000412		0.0032195		0.000667		0.0009958	
Deforestation during transition [ha]	970		83		2,755		3,807		2,838	
Annual rate [ha/yr]	97		8		276		381		284	

Annex 2: Correlation of driver proxies

First_Variable*	Second_Variable*	Chi_2	Crammer	Contingency	Joint_Entropy	Joint_Uncertainty
Proxies/Altitude	Proxies/Vegetation	3149970.68	0.268208861	0.646829355	3.912444288	0.141797208
Proxies/Distance_to_provincial_capital	Proxies/Distance_to_roads	6319737.48	0.086908219	0.771755844	5.863815754	0.132135277
Proxies/Altitude	Proxies/Distance_to_coastline	3059660.35	0.265013623	0.642313895	4.378377945	0.127754786
Proxies/Distance_to_roads	Proxies/Distance_to_settlements	2903931.15	0.107094158	0.635282143	4.252433399	0.112677768
Proxies/Distance_to_provincial_capital	Proxies/Vegetation	3503871.57	0.25877184	0.667487314	5.722334673	0.096780464
Proxies/Altitude	Proxies/Slope	1278998.85	0.222212908	0.478075984	3.508743097	0.088427874
Proxies/Distance_to_coastline	Proxies/Vegetation	1669985.1	0.178720732	0.526390978	4.378305459	0.081218744
Proxies/Distance_to_roads	Proxies/Vegetation	1528629.68	0.172682471	0.513352929	4.182090935	0.080076861
Proxies/Distance_to_coastline	Proxies/Distance_to_provincial_capital	2166338.54	0.075920656	0.575687797	6.254444407	0.074112975
Proxies/Altitude	Proxies/Distance_to_roads	1380595.65	0.179782585	0.494233247	4.326408392	0.067464869
Proxies/Distance_to_coastline	Proxies/Distance_to_settlements	1404686.88	0.073798169	0.493136249	4.554683071	0.067326299
Proxies/Slope	Proxies/Vegetation	945146.237	0.191077079	0.423907594	3.429644591	0.06666614
Proxies/Altitude	Proxies/Distance_to_provincial_capital	1632486.42	0.193501454	0.521943166	5.94361897	0.060594997
Proxies/Distance_to_provincial_capital	Proxies/Distance_to_settlements	1850788.51	0.084629095	0.545016887	5.977405	0.058912666
Proxies/Distance_to_coastline	Proxies/Distance_to_roads	1161528.36	0.056162635	0.461932685	4.705900608	0.057398275
Proxies/Distance_to_roads	Proxies/Slope	832523.167	0.181526712	0.406293639	3.731173175	0.053994706
Proxies/Altitude	Proxies/Distance_to_settlements	1049784.9	0.155147388	0.440463405	4.23168052	0.053790488
Proxies/Distance_to_settlements	Proxies/Vegetation	830832.311	0.125989568	0.40000376	4.13133572	0.048733836
Proxies/Distance_to_provincial_capital	Proxies/Slope	933805.949	0.190324868	0.422537228	5.34604729	0.044769873
Proxies/Distance_to_settlements	Proxies/Slope	321979.619	0.11174392	0.26400455	3.65760814	0.021117603
Proxies/Distance_to_coastline	Proxies/Slope	248000.663	0.098124735	0.233699798	3.998710393	0.014441485